

Yu, Z., Mao, X., and Jaworski, A. J. (2014) Experimental study of heat transfer in oscillatory gas flow inside a parallel-plate channel with imposed axial temperature gradient. *International Journal of Heat and Mass Transfer*, 77, pp. 1023-1032.

Copyright © 2014 Elsevier, Ltd.

A copy can be downloaded for personal non-commercial research or study, without prior permission or charge

Content must not be changed in any way or reproduced in any format or medium without the formal permission of the copyright holder(s)

<http://eprints.gla.ac.uk/97983/>

Deposited on: 16 April 2015

Heat transfer in an oscillatory gas flow inside a parallel-plate channel with imposed axial temperature gradient

Zhibin Yu, Xiaolan Mao and Artur J. Jaworski¹

Department of Engineering, University of Leicester
University Road, Leicester LE1 7RH, UK

¹ Corresponding author: a.j.jaworski@leeds.ac.uk; T: +44(0)113 343 4871

Abstract

Understanding of heat transfer processes between a solid boundary and an oscillatory gas flow is important for the design of internal components such as heat exchangers, regenerators and thermal buffer tubes in thermoacoustic and Stirling thermodynamic machines where the flow oscillations are part of the power production or transfer processes. The heat transfer between the flow and an arrangement of hot and cold plates forming a parallel-plate channel is studied experimentally and numerically. Here, the particular focus is on the processes occurring within the thermal and viscous boundary layers. The measured phase-dependent temperature fields combined with the velocity fields are studied in detail. Near wall temperature minima and maxima of the cross sectional temperature profiles are observed when the gas moves from cold to hot or from hot to cold parts of the channel. They are referred to as "temperature undershoot" and "overshoot", respectively. The existence of these temperature minima and maxima causes large local temperature gradients in the direction normal to the wall, which result in large heat diffusion between gas layers in the direction normal to the wall. It is observed that the flow history has a strong impact on the temperature fields. This invalidates the so-called "Iguchi hypothesis", based on which the heat transfer data for steady flows is being applied to oscillatory flow conditions. General guidelines for the design of heat exchangers used in thermoacoustic devices are discussed.

Keywords: Oscillatory flow, Heat transfer, Heat exchanger, Thermoacoustic

1. Introduction

Heat transfer processes in the presence of oscillatory flows have received a lot of research interest in the past few decades. The heat transfer enhanced due to the oscillatory flow may lead to a large variety of possible applications. Therefore a large number of experimental and numerical works have been carried out, and some examples are given in Refs. [1-8]. On the other hand, a variety of devices such as Stirling engines or coolers, thermoacoustic devices and pulse tube coolers employ the oscillatory gas flow of the working fluid as a means of energy transfer. Therefore, the design of heat exchangers, stacks/regenerators and thermal buffer tubes in such devices requires the understanding of the heat transfer process between the solid boundary and oscillatory gas flow.

General reviews of the heat transfer processes in the presence of oscillatory flow have been given by Cooper et al. [9], Zhao and Cheng [10], and Sert and Beskok [11]. Kurzweg and Zhao [12] and Kurzweg [13, 14] have been first to develop a concept of the so-called “dream pipe”, which used the sinusoidal oscillation of water flow to enhance the heat transfer in a pipe between the cold and hot reservoirs. The mechanism of this enhancement was attributed to: (i) the phase lag occurring between the fluid in the centre and that near the wall; and (ii) transverse heat transfer between these two parts of fluid, and the enhanced axial heat transfer due to the oscillatory displacement of the fluid along the pipe [12-13].

Subsequently, Zhao and Kurzweg [15] also conducted numerical simulations of their dream pipe. Neglecting the motion of the fluid within the penetration depth in the near wall region, they treated this part of fluid as a thermal capacity for heat accumulation. The penetration depth due to thermal diffusion is defined as $\sqrt{2\kappa/\omega}$, with κ being the thermal diffusivity and ω the angular frequency of the oscillation. Ozawa and Kawamoto [16] pointed out that such a treatment did not account for the time-dependent temperature profiles near the channel wall. They developed a lumped-parameter heat transfer model to simulate the dream pipe with water as working fluid at a frequency of less than 1 Hz. The simulations agreed with the time-dependent temperature fields in the dream pipe qualitatively (the temperature being measured using a thermo-sensitive liquid-crystal tracer technique). Their research showed that the isotherms change significantly from the shape of upward peak to that with a downward peak. The change of the isotherm's shape followed that of the velocity profile with a certain phase lag. In addition to Zhao and Kurzweg's understanding of the mechanism of heat transfer enhancement mentioned above, Ozawa and Kawamoto [16] revealed that the transverse diffusion of heat due to the radial temperature gradient caused by the phase lag

of the fluid motion between the fluid in the channel centre and near the wall also played an important role in such heat transfer enhancement.

Zhao and Cheng [17] investigated a laminar oscillatory flow in a heated pipe numerically. An “annular effect” in the temperature profiles near the entrance of the pipe was observed. This is characterised by a temperature minimum or maximum near the wall rather than at the centre of the flow channel, when the wall is at a temperature higher or lower than the bulk flow. This annular effect in the temperature profiles becomes more pronounced with the increase of the kinetic Reynolds number, $Re_\omega = \omega D^2/\nu$, where D is the channel width and ν is the fluid kinematic viscosity. The presence of the annular effect was also verified by the numerical simulation of an oscillatory flow in a channel carried out by Sert and Beskok [11]. In their model, the middle portion of the top plate was uniformly heated and its two sides were kept at a constant temperature, while the bottom plate was insulated. It was reported that for an oscillatory flow with a Womersley number ($\alpha = \sqrt{\omega D^2/\nu}$) of 10, large cross-sectional temperature variations were observed in the temperature fields, which are much less significant in the temperature fields when the Womersley number is at 1 when the annular effect in the velocity profiles is not present. It was understood that these temperature distributions in the channel were highly affected by the velocity profile. It is immediately clear to see that the Womersley number is the square root of the kinetic Reynolds number, Re_ω . The forced convection due to the flow motion increases with the increase of the penetration depth, Womersley number and Prandtl number (ratio of momentum and thermal diffusivities). Furthermore, they reported that the corresponding steady unidirectional forced convection was even more effective than the oscillatory flow forced convection for the tested case. It seems that the abovementioned “annular effects” represent the same kind of phenomena as the so-called upward and downward peaks in isotherms observed by Ozawa and Kawamoto [16].

Liao et al. [2] applied a channelled oscillatory air flow to cool microprocessor chips. They reported that there are two different heat transfer enhancement mechanisms. When the Reynolds number, $Re = U_m D/\nu$ defined on the maximum velocity of the imposed oscillatory flow, is small, the heat transfer enhancement is mainly due to the reduction of Stokes' layer thickness, $\sqrt{2\nu/\omega}$, with the increase of the oscillation frequency. While in the high Reynolds number region, the heat transfer is enhanced due to the presence of the higher-order harmonics of imposed flow frequency. Li and Yang [18] investigated numerically the heat transfer in reciprocating flows at low frequencies and large amplitudes in short channels. They demonstrated a heat transfer enhancement due to the intra-cycle oscillations at the inlet and exit of the flow channels, which is likely caused by flow

separation. The intra-cycle oscillations were characterised by the axial velocity oscillations within individual cycles, especially during the accelerating stage.

As can be seen, substantial progress has been made in understanding the mechanisms behind the enhanced heat transfer in oscillatory flow. However it is also clear that such understanding is still incomplete, in particular in terms of a simultaneous analysis of the time-resolved temperature and velocity fields. Notably, previous research has been conducted to measure the overall heat transfer coefficients in heat exchangers subjected to oscillatory flow for different specific applications [7, 19-22] and thus it did not consider the microscopic fluid flow and heat transfer behaviour. Very few experimental research studies [16, 23-25] focused on the time-resolved temperature fields in oscillatory conditions for some particular applications, however these did not attempt to combine the temperature and velocity field (or fluid displacement) information.

It is also worth noting that most of the experimental studies mentioned above have been conducted with incompressible fluids, such as liquid water, which has Prandtl number greater than 1. This makes the viscous boundary layer thicker than the thermal boundary. As discussed above, the heat transfer enhancement in oscillatory flow is mainly due to the interactions between the thermal and viscous boundary layers. It remains unclear of how the effect of the Prandtl number on the heat transfer processes is different in the cases when gases are used as the flow medium. Therefore, it would be interesting to explore such interactions for a compressible medium (e.g. gas) in order to mimic the actual situation encountered in thermoacoustic devices, Stirling engines and pulse tube coolers.

The main objective of this work is to examine the time-dependent velocity and temperature fields obtained experimentally in order to gain a better understanding of heat transfer processes in thermoacoustic heat exchangers. In their previous work [26, 27] the authors demonstrated the use of Planar Laser Induced Fluorescence (PLIF) and Particle Image Velocimetry (PIV) techniques to measure time-dependent temperature and velocity fields, respectively, within a heat exchanger in a thermoacoustic system. Here, these techniques are applied to acquire the velocity and temperature fields in a parallel-plate channel in an oscillatory gas flow of one oscillation amplitude at a single frequency. Due to the limitation of the current experimental setup, numerical simulation has been developed to extend this examination to cover a range of oscillation amplitudes and operating frequencies.

Furthermore, on the engineering design level, this research aims to provide further guidance to aid the design of heat exchangers in thermoacoustic systems. The current practice, based on the Iguchi

hypothesis (i.e. each instant of the time-dependent flow depends only on that instant's velocity, not on the flow history), is to use the data obtained for steady flows for the design of heat exchangers for oscillatory flows [28, 29]. The Iguchi hypothesis is confirmed to be applicable at some conditions when the oscillation amplitude is relatively large [30, 31]. However, as the displacement of the gas is comparable with the length of the heat exchanger, one might question the validity of this hypothesis. In this paper, this issue is also discussed on the basis of the obtained experimental results. Furthermore, the principles of the heat exchanger design for thermoacoustic systems will also be discussed.

2. Experimental method

The detailed description of the test rig and the experimental and measurement procedures can be found in the already mentioned previous work [26, 27] and therefore only a brief description will be provided here. Figure 1a is a schematic illustration of the experimental apparatus. It is essentially a 7.4 m long quarter-wavelength resonator where the intensity of the acoustic excitation (and thus fluid displacement amplitude) is controlled by the level of excitation provided by a loudspeaker (sub-woofer). The resonator has a rectangular cross-section with internal dimensions 134 mm by 134 mm. The operating frequency of the test rig is 13.1 Hz.

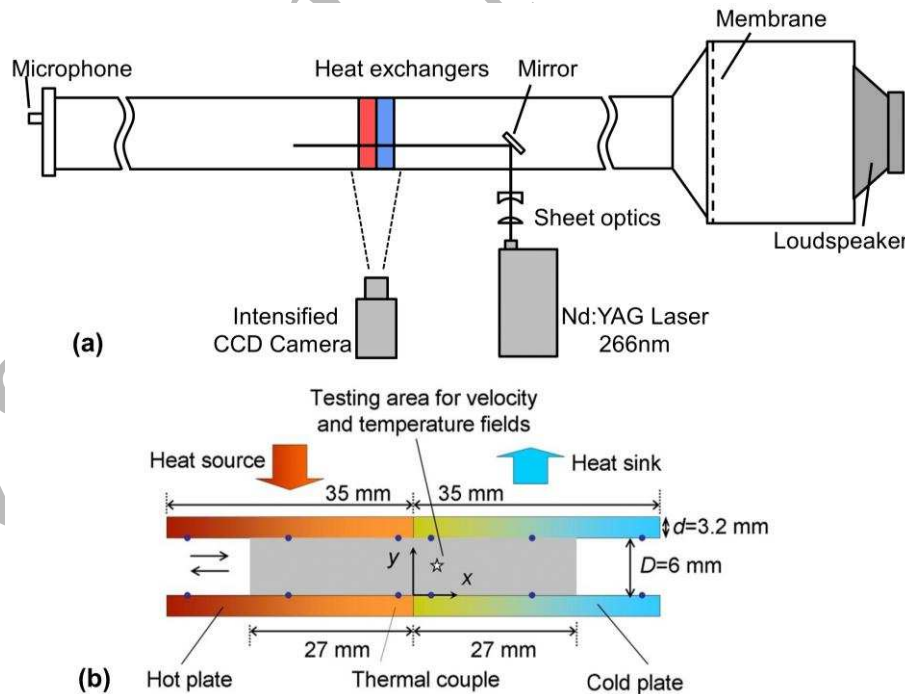


Figure 1 (a) Schematic illustration of the experimental apparatus with PLIF system deployed (similar setup for PIV is omitted); (b) close up of the test channel formed by a pair of “hot” and “cold” plates within the heat exchangers

A pair of parallel-plate heat exchangers is placed inside the resonator, 4.6 m from the end plate shown in Figure 1a, where the acoustic anti-node exists [27]. The “hot” heat exchanger is constructed from a series of brass plates, each containing an embedded cable heater, used to control the plate temperature. The “cold” heat exchanger is constructed from a series of plates containing a meandering channel for cooling water. Both hot and cold plates have a length (l) of 35 mm along the axial direction of the resonator, a width (w) of 132 mm in the transverse direction, and a thickness (d) of 3.2 mm. The plates form a series of channels with a height (D) of 6 mm, and one of them is schematically depicted in Fig. 1b. As a result, the Womersley number for the flow in these channels is between 9.2 and 13.4, and the kinematic Reynolds number is in the range of 85–180, due to the temperature dependent kinematic viscosity.

Twelve fine-wire K-type thermocouples (marked as dots in Fig. 1b) are placed on the surface of hot and cold plates forming the test channel. There are three pairs on cold plates. They are 3.0, 17.5 and 32.0 mm away from the joint (i.e. $x = 0$), respectively. Symmetrically to the joint, there are also three pairs on the hot plates as shown in Fig. 1b. The thermocouples monitor the temperature distribution on the hot and cold plates. A PID temperature controller (Omega Model CN8592) is used to accurately control the temperature at the reference point ($x = -32\text{mm}$, $y = 6\text{ mm}$) to within $\pm 1\text{ }^{\circ}\text{C}$ at a pre-set value of $200\text{ }^{\circ}\text{C}$ for the experiments in this paper. The cold plates are cooled to around $30\text{ }^{\circ}\text{C}$.

The arrangement described above allows obtaining oscillatory gas flow within the test channel, maintained by the acoustic excitation. The measurement methodologies adopted in this work include two-dimensional temperature and velocity field measurements using Planar Laser Induced Fluorescence (PLIF) and Particle Image Velocimetry (PIV), respectively. By these means, the temperature and velocity fields within the channels can be obtained and thus the heat transfer between the oscillatory gas flow and the cold and hot plates can be studied.

Generally, the rationale behind the current experimental arrangement is to use the hot and cold plates to mimic the fins of respective heat exchangers that are often part of heat engines which employ oscillatory gas flow, e.g. thermoacoustic engines, pulsed tube coolers or Stirling engines. In the channels shown in Fig.1b, the hydraulic radius, r_h , defined as ratio of the gas volume to the wet area, is 3 mm. It is of the same order of the thermal penetration depth ($\delta_k = \sqrt{2\kappa/\omega}$) and viscous penetration depths ($\delta_v = \sqrt{2\nu/\omega}$). These two characteristic lengths are often used with oscillatory flows to indicate the distance heat and momentum can diffuse transversely during the time interval

of $1/\omega$ [32]. They are used as approximate criteria for determining the fin spacing [29]. The thermal penetration depth, δ_k , is in the range of 0.7–1.2 mm, and the viscous penetration depth δ_v in the range of 0.6–1.0 mm along the channel, when the temperature dependent thermal diffusivity and kinematic viscosity of air are considered.

It is interesting to note that the two heat exchangers were placed side by side without any gap in the x direction, mainly to simplify the arrangement for the ease of laser illumination and avoid shadow between the adjacent hot and cold plates. Clearly, such an arrangement introduces an unwanted heat flux from the hot to the cold plates through heat conduction. As a consequence, the surface temperature on the hot and cold plates gradually decreases from the left to the right as indicated in Fig. 2a. This also leads to a nonlinear temperature distribution within the gas, with a steep temperature change in the vicinity of the joint due to the temperature difference between the hot and the cold plates (Fig. 2b).

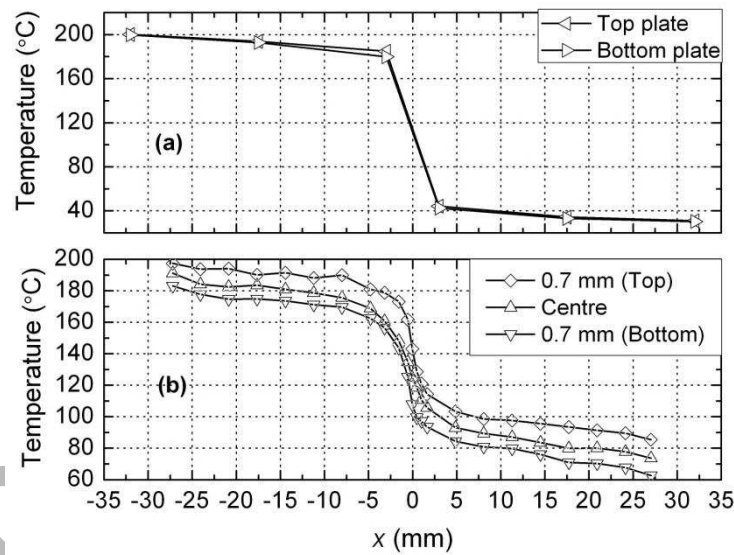


Figure 2 (a) Temperatures on the hot and cold plates; (b) Temperature profile along the channel in static air in thermal steady state.

In the experiments, the phase locking circuit uses the pressure signal detected by the microphone installed on the end cap of the acoustic resonator as reference signal to trigger the PLIF and PIV system in order to take the measurements at selected time instants in an acoustic cycle. The details of how the phase locking mechanism works can be found for example in previous work [27]. The flow velocity amplitude (u) within the test channel can be controlled by adjusting the acoustic excitation of the loudspeaker. The time-resolved velocity field in the test channel was accurately

measured by PIV. The measured velocity, u , can be converted to the gas parcel displacement, ξ , using $\xi = u/\omega$, with the velocity leading the displacement by 90° in phase. In this paper, it is often more convenient to discuss the measurement results with reference to the displacement rather than the velocity. Figure 3 shows the measurement points represented as phase angle within the acoustic cycle (measurements taken every 18° , i.e. 20 measurements in the cycle) and the corresponding displacement ξ . The results presented in this paper are based on the displacement amplitude ξ_a of 17 mm. The reference point is at a location with reference to the gas parcel displacement in an acoustic cycle, which is calculated from the velocity measured at the point ($x = 5.0$ mm, $y = 3.0$ mm) marked by a star in Fig. 1b. In principle, every point in the channel can be chosen and similar displacement curves to the one shown in Fig. 3 can be plotted. However, for the convenience of analysis of the cross sectional temperature profiles in the following sections, this particular point was chosen as a reference.

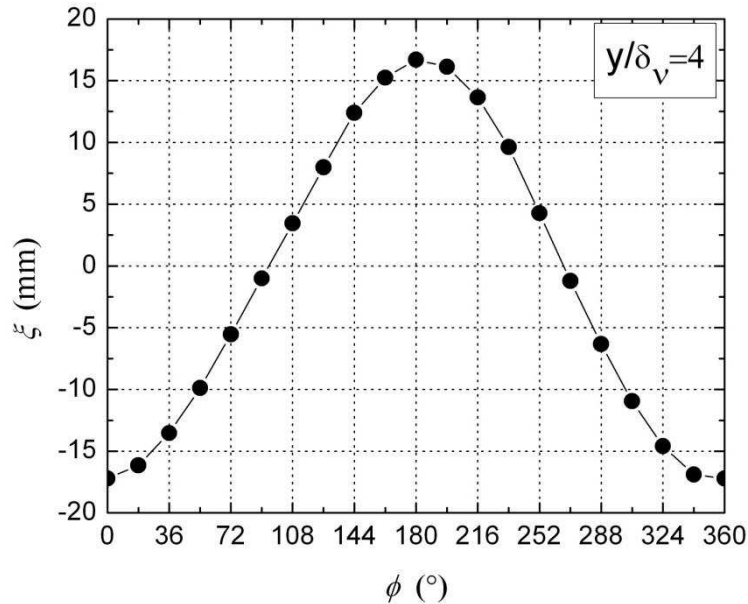


Figure 3 Displacement versus phase angle for the results presented

3. Experimental results and discussion

The results presented in this section are grouped in five subsections. Section 3.1 summarises the results of phase-dependent temperature fields obtained within the one acoustic cycle. Sections 3.2 and 3.3 are focused on the phenomena of temperature “overshoot” and “undershoot”, respectively. Section 3.4 discusses the obtained phase-dependent velocity and displacement profiles, while Section 3.5 discusses further the experimental results in several aspects, that is, the interaction of velocity and temperature fields, the effect of the “flow history” on the oscillatory flow behaviour and the effects of temperature overshoot/undershoot on the heat transfer. This is followed by

Section 4 containing the results from a numerical study of the same arrangement in a number of flow oscillation amplitudes and frequencies.

3.1 Temperature fields in one acoustic cycle

Figure 4 shows the two-dimensional temperature field distribution in the cross-section parallel to the flow direction for 20 phases obtained for the displacement amplitude ξ_a of 17 mm. At phase $\phi = 0^\circ$, the fluid displacement reaches the negative maximum value, which means that the gas parcel in the channel moves farthest to the left (as can be inferred from Fig. 3). It can be seen that, at this instant, the cold gas moves into the hot channel. However, this penetration is only pronounced in the central area of the channel. Adjacent to each hot plate, there is a thin layer of gas with high temperature, which seems not to be affected by the cold gas coming from the cold channel.

After this phase, the gas parcel starts to accelerate to move to the right. From phase $\phi = 0^\circ$ to $\phi = 90^\circ$ the gas moves from the displacement farthest left into the equilibrium location as shown in Fig. 3. From the temperature image, it can be found that the cold gas gradually flows out from the hot channel after being partially heated. The hot gas, which was heated and has been pushed out from the hot channel at the end of the previous acoustic cycle, gradually takes over the left end of the hot channel. From phase $\phi = 18^\circ$ to $\phi = 90^\circ$, it can be observed that two layers of gas with relatively high temperature (as shown in orange) gradually penetrate into the cold channel. It can be found that these two layers of gas have higher temperatures than those of the gas either in the centre of the channel or adjacent to the cold plates. As a result, a temperature maximum is present in this layer, rather than at the centre of the channel or on the wall. This feature of the temperature field is referred to as "temperature overshoot".

At phase $\phi = 90^\circ$, the gas reaches the equilibrium position, and the velocity reaches the maximum. After this time instant, the gas starts to move to the right while beginning to decelerate. It can be seen that the central area at the right of the hot channel still shows relatively low temperatures at this phase. This indicates that during the preceding quarter of the acoustic cycle ($\phi = 0-90^\circ$), the heat transfer from the hot plate to the gas has not influenced the gas temperature in the central area significantly. The "temperature overshoot" effect seems very strong at phase $\phi = 90^\circ$ and becomes even more pronounced at $\phi = 108^\circ$ and $\phi = 126^\circ$. Subsequently, the effect weakens and practically disappears at phase $\phi = 180^\circ$. From Fig. 4, it can be seen that most of the cold channel is still occupied by the gas with relatively low temperature. This implies that the gas has not been heated

substantially when it was previously present in the hot channel during phases between $\phi = 0$ and 90° .

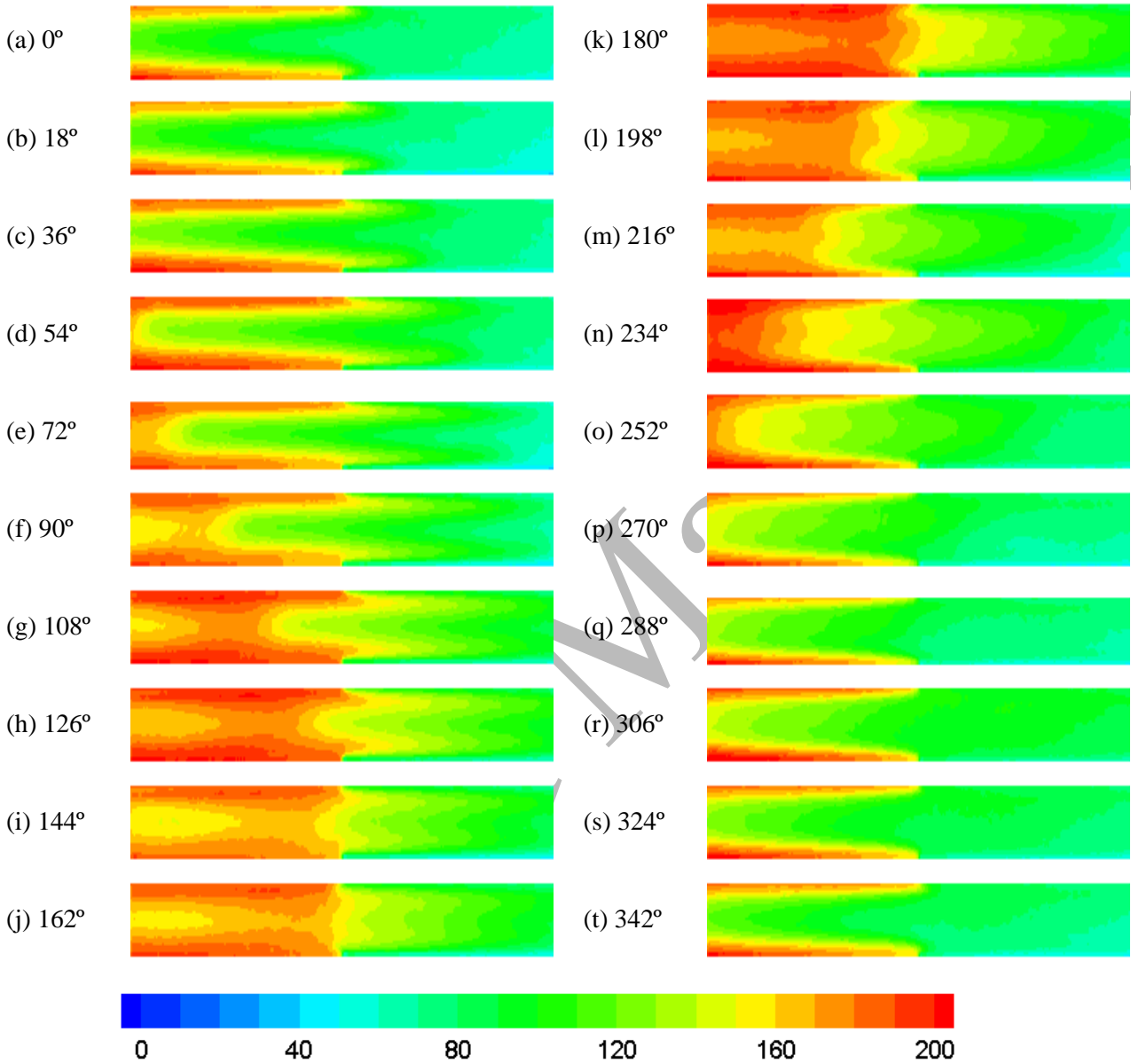


Figure 4 Time dependent temperature fields in the test channel (temperature scale in degrees Celsius)

At phase $\phi = 180^\circ$, the gas reaches farthest to the right in the channel. After this instant, the gas starts to move to the left, reaching the equilibrium position by phase $\phi = 270^\circ$. The gas transfers heat to the cold plates during this period. By inspecting the temperature fields (c.f. the right end of the hot channel) for phases $\phi = 198^\circ$, 216° and 234° , one can find interesting patterns of “temperature undershoot”, i.e. a somewhat opposite effect to the “temperature overshoot” where a temperature minimum occurs in the gas that is neither adjacent to the wall nor in the centre of the channel. This “temperature undershoot” disappears completely at phase $\phi = 270^\circ$. From phase $\phi = 288^\circ$ to $\phi =$

342°, the gas accelerates to move to the left end of the channel. After it reaches the farthest left end ($\phi = 360^\circ$ or $\phi = 0^\circ$), it enters the next acoustic cycle.

It should also be noted that, the temperature fields are slightly asymmetric relative to the centreline of the channel. This is mainly due to the accumulated residual heat in the void space in the resonator to the left of the hot plates. This is caused by the natural buoyancy effect over time, often an hour or so that is necessary for the calibration and measurement using PLIF technique. This asymmetry can also be seen from the gas temperature profiles along the channel in Fig.2 – the gas near the top plate is slightly hotter than that close to the bottom plate.

3.2 Temperature profiles of "temperature overshoot"

As shown in Section 3.1, the "temperature overshoot" effect only exists in the cold channel when the gas flows to the right. It will be interesting to investigate further the phase-dependent cross-sectional temperature profiles within the cold channel within this type of flow. Following the normalisation proposed by Zhao and Cheng [10], the normalised fluid temperature is expressed as

$$\theta = \frac{T_f - T_w}{T_H - T_C} \quad (1)$$

where θ , T_f , T_w , T_H and T_C are normalised fluid temperature, local fluid temperature, wall temperature, reference hot temperature (here 200 °C), reference cold temperature (here 30 °C), respectively. The distance from the bottom plate, y is normalised using the viscous penetration depth, δ_v . An average viscous penetration depth (i.e. $\delta_{v,a} = 0.75$ mm) is used as the characteristic length.

Fig. 5 shows the normalised temperature profiles for ten selected phases at a location 5.0 mm away from the joint into the cold channel ($x = 5.0$ mm). For simplicity, only the temperature profiles at the bottom half of the channel are presented. At $\phi = 0-90^\circ$, the temperature profiles have peaks with $y/\delta_{v,a}$ less than 1, while the gas moves from the left to its equilibrium position with increasing speed. The peak temperature is substantially higher than the gas temperature in the channel centre. With the gas moving further right, the temperature peak moves away to the centre and reaches $y/\delta_{v,a} = 2$ when $\phi = 162^\circ$. Further on, the temperature peak continue to shift to the centre, and the peak temperature starts to decrease ($\phi = 198^\circ$ and 234°); the gas temperature in the channel centre reaching the maximum at $\phi = 198^\circ$. The temperature profiles generally have a maximum somewhere

in between the wall and the centre, but the "temperature overshoot" described above is much less recognisable when the gas moves from the right to the left ($\phi = 198\text{--}342^\circ$).

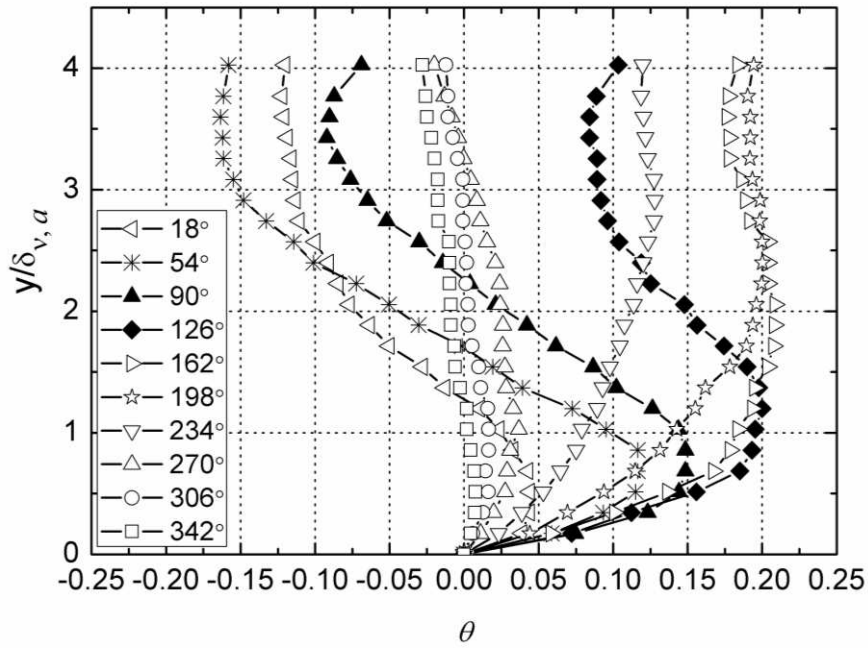


Figure 5 Cross-sectional temperature profiles for ten selected phases ($x=5.0$ mm). The temperature maxima near the wall for phases $\phi = 90^\circ$ and $\phi = 126^\circ$ (in solid symbols) can be seen.

Fig. 4 also shows that the temperature overshoot effect is very apparent near the joint between “cold” and “hot” channel, while it seems weaker further to right of the cold channel. However, it is difficult to judge from Fig. 4 whether there is a dependence of the temperature overshoot effect on the location. Therefore, for the purpose of further analysis, the temperature profiles at different locations, for a selected phase $\phi = 90^\circ$ have been extracted and plotted as Fig. 6. Five locations have been selected along the cold channel from left to the right with x changing from 5 mm to 25 mm with a step of 5 mm. It can be found from Fig. 6 that the shape of the individual temperature profiles is quite similar, while the location of the temperature peak moves slightly below $y/\delta_{v,a} = 1$ to slightly above. The magnitude of the temperature overshoot effect seems to differ from location to location. However, from Fig. 2, one can hypothesize that this dependency is mostly likely due to the nonlinear temperature profile along the channel. One can see that the temperature gradient dT_m/dx decreases when x increases from 5 mm to 25 mm. This will be discussed further in Section 3.5.

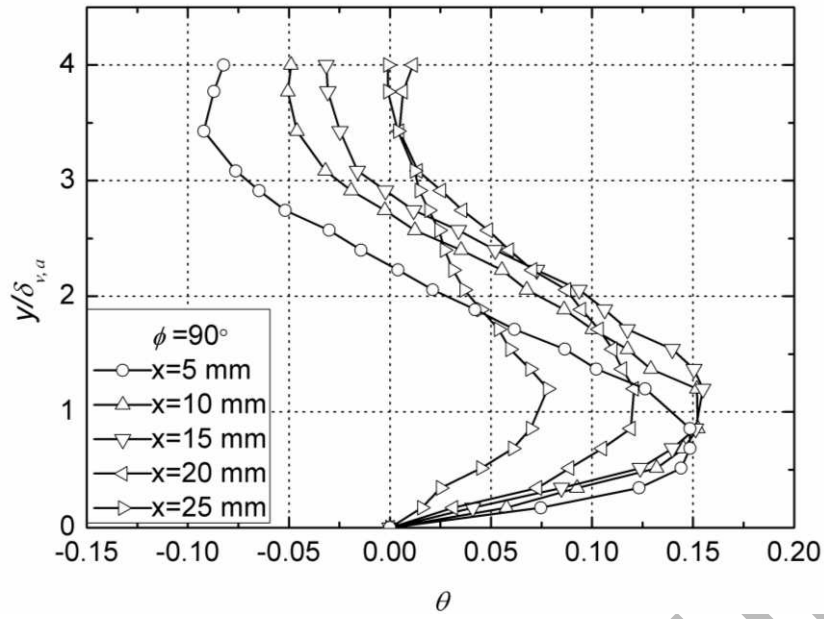


Figure 6 Cross sectional temperature profiles for different locations along the cold channel ($\phi = 90^\circ$).

The temperature peaks shown in Fig. 5 indicate that the gas temperature at the peak point is considerably higher than those near the centre and plate surface. Therefore, it would be interesting to find out the actual temperature differences from the data before normalisation. Figure 7 shows the extracted temperature differences between the maximum temperature of each profile T_{\max} and the temperature in the centre of the channel T_{centre} . For convenience of comparisons, it is also plotted against location given in the legend of Fig. 6. It can be found that, the temperature difference is around 41 °C for $x = 5.0$ mm and it decreases to around 13 °C for $x = 25.0$ mm.

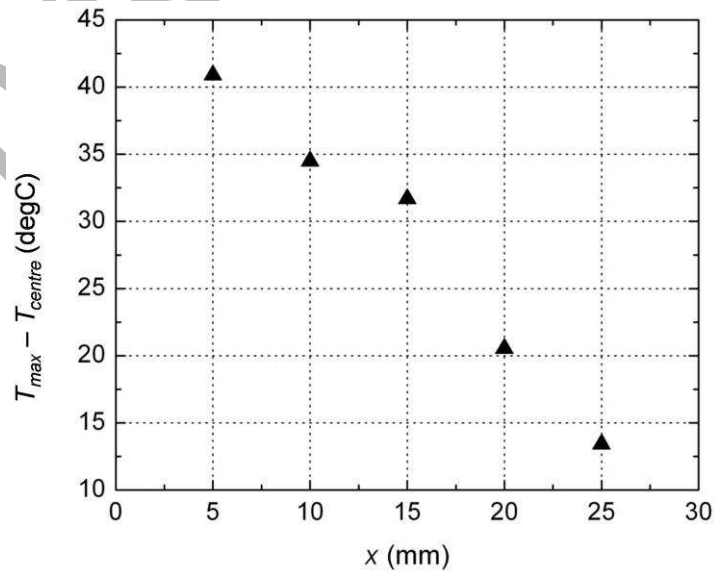


Figure 7 Difference between the maximum temperature and the temperature in the channel centre for each temperature profile shown in Figure 6 plotted against location x .

3.3 Temperature profiles of “temperature undershoot”

As already mentioned in Section 3.1 the effect of “temperature undershoot” exists in the hot channel when the gas flows to the left. In an analogous way as that described in Section 3.2, the phase-dependent temperature profiles of the cross sectional temperature fields in the hot channel can be extracted. Fig. 8 shows such normalised phase temperature profiles at location $x = -5.0$ mm. The temperature profiles exhibit an apparent minimum for $y/\delta_{v,a} \sim 1$ for phases of $\phi = 198^\circ$ and $\phi = 234^\circ$. However, these local temperature minima are not as pronounced as temperature maxima shown in Fig. 5. For phase $\phi = 234^\circ$, the difference between the gas temperature at the channel centre and the temperature minimum is only around 10°C .

Following the same methodology as used in Fig. 6, the temperature profiles at different x locations at phase $\phi = 234^\circ$ have been extracted and plotted in Fig. 9. Five locations have been selected along the hot channel from left to the right with x changing from -25 mm to -5 mm with step of 5 mm. It can be found from Fig. 9 that the temperature undershoot effect is observed at locations $x = -5.0$, -10.0 and -15.0 mm, but not at locations $x = -20.0$ and -25.0 mm.

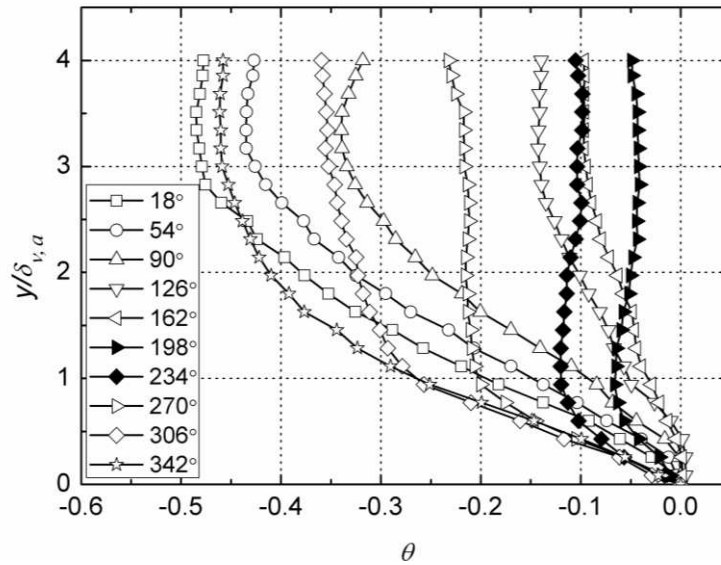


Figure 8 Cross sectional temperature profiles for ten selected phases ($x = -5.0$ mm). The temperature minima near the wall can be seen for phases $\phi = 198^\circ$ and $\phi = 234^\circ$

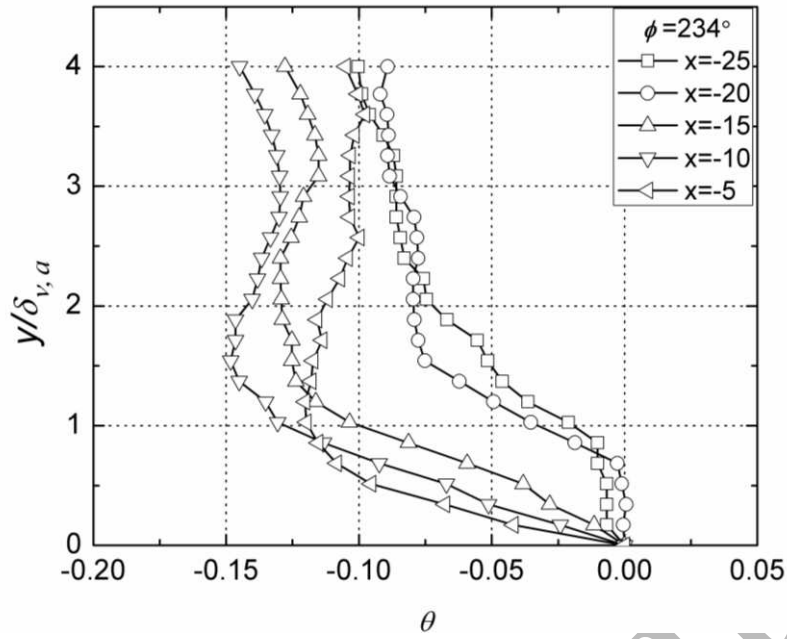


Figure 9 Cross sectional temperature profiles for different locations along the hot channel ($\phi = 234^\circ$)

3.4 Phase-dependent velocity and displacement profiles

The experimental results discussed so far suggest that the instantaneous displacement of the gas parcels belonging to different “layers” of fluid (i.e. of different y distances away from the solid wall) is important for understanding the heat transfer processes between the fluid and the plate. As described in Section 2, the velocity field measurements were performed for 20 phases in an acoustic cycle. Fig. 10 shows the cross sectional velocity profiles for $x = 5.0$ mm, for all investigated 20 phases. Of course the amplitude of velocity depends on y . It increases from 0 to the maximum as y increases from 0 to around $2.5\delta_{v,a}$, and then slightly decreases as y approaches the centre of the channel. These “overshoots” of velocity are also known as “annular” effects and have been well documented in the literature related to oscillatory flow, e.g. [17].

Similarly, when looking at profiles for individual phases in the cycle, one can see that the velocity of gas parcels also depends on y . However it can also be seen that for two different values of y (i.e. for different fluid “layers”) the instantaneous values of velocities can have a relative phase lag – for example for phase $\phi = 0^\circ$ and parcel at $y = \delta_{v,a}$ it is positive, while in the channel centre it is negative; and an opposite is true for phase $\phi = 180^\circ$. Furthermore, as the temperatures at two sides of the selected x location (here $x = 5$ mm) are different, the gas experiences different viscous drag because the viscosity depends on the gas temperature. Similarly, the fluid density is a function of

temperature and this can cause asymmetries in the positive and negative displacement values. For these reasons the “bundle” of the phase-dependent velocity profiles appears as a slightly asymmetric pattern in Fig. 10.

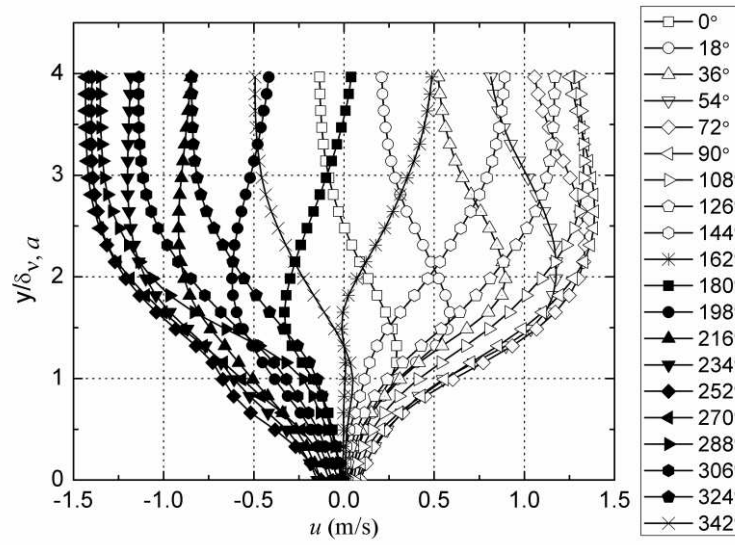


Figure 10 Phase-dependent velocity profiles as function of y ($x=5.0$ mm)

Clearly, the velocity profiles can be converted into phase-dependent displacement profiles of the gas parcels. The converted results are shown in Fig. 11 and illustrate the Lagrangian point of view of looking at individual parcels and their displacement from equilibrium. It should be noted that, there is a 90° phase difference compared to the velocity. Obviously, the displacements show the same dependence on y . Fig. 11 also shows that there is a phase lag between different layers of gas.

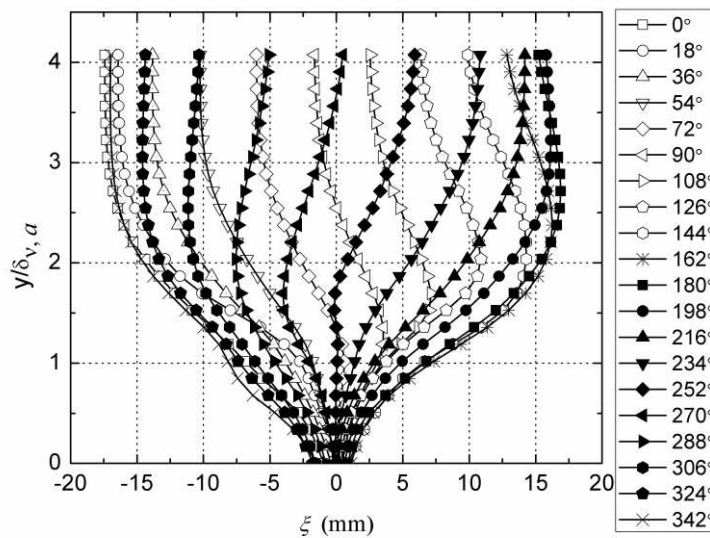


Figure 11 Phase-dependent displacement profiles as function of y ($x=5.0$ mm)

3.5 Discussion

Some of the important aspects of the discussion of the presented experimental results are the issues of the interactions between the velocity and temperature fields; the related influence of “flow history” on the flow behaviour; and the effects of over-/undershoots on the heat transfer. These are considered in the following subsections.

3.5.1 Interaction of velocity and temperature fields

To better understand the underlying thermo-fluid mechanisms behind the temperature overshoot/undershoot effects, it is helpful to compare selected temperature fields with the results shown in Figs. 5 and 11. To this end, Fig. 12 illustrates “magnified” temperature fields obtained for phases $\phi = 108^\circ$ (Fig. 12a) and $\phi = 234^\circ$ (Fig. 12b). Gridlines, with the relative distance between them of $\delta_{v,a} = 0.75$ mm have been added to the temperature fields to help the discussion.

Looking at Fig. 12a, one can identify a thin layer of warm gas (denoted by orange colour, located approximately between $y = \delta_{v,a}$ and $y = 2\delta_{v,a}$) which penetrates into the cold channel. However, it can also be seen that the layer of gas adjacent to the surface of the cold plate ($y < \delta_{v,a}$) remains relatively cold (as illustrated by green colour). Similarly, looking at Fig. 12b, it can be seen that a thin layer of cold gas (denoted by green colour, located approximately between $y = \delta_{v,a}$ and $y = 2\delta_{v,a}$) penetrates into the hot channel. However, it can also be seen that the layer of gas adjacent to the surface of the hot plate ($y < \delta_{v,a}$) remains hot (as illustrated by red colour).

Looking at Fig. 11, one can find that the displacement of gas within the layer where $y < \delta_{v,a}$ is in the range of 5–6 mm taking the middle of the layer as reference. This means that most of fluid in this layer has not travelled to the hot (cold) channel during the previous phases. Therefore, it is cooled (heated) by the cold (hot) plate all the time. On the other hand, the gas in centre of the channel (say $y > 3\delta_{v,a}$) is not affected by the viscous drag effects from the wall. It moves with a higher displacement amplitude. This part of gas is also not affected by the thermal diffusion from the wall. Therefore, it practically keeps the temperature obtained from the static conditions. However, the gas located between $y = \delta_{v,a}$ and $y = 3\delta_{v,a}$ exhibits a much more complicated behaviour. For this part of gas, the amplitude of displacement and changes in temperature both strongly depend on y . A qualitative analysis of Figs. 11 and 12 suggests that this layer of gas moves with relatively high displacement, but is also affected by the thermal diffusion from the wall. Therefore, the fluid can be partially heated up when it is present in the hot channel (from $\phi = 0^\circ$ to $\phi = 180^\circ$), and can be cooled down during its presence in the cold channel (from $\phi = 180^\circ$ to $\phi = 360^\circ$). From the Lagrangian point of view, the local temperature maximum can occur when the gas moves from the cold channel

to the hot channel (i.e. the temperature overshoot shown in Fig. 12a), and local temperature minimum (i.e. the temperature undershoot shown in Fig. 12b) can occur when the gas moves from the cold to the hot channel. In addition, when looking at the displacement as a function of phase angle for the fluid where $y > 3\delta_{v,a}$ and $y < 3\delta_{v,a}$ one can see that there is a relative phase difference for the fluid near the centre and closer to the wall.

The current observations strongly suggest the temperature overshoot and undershoot effects documented in this paper are essentially similar phenomena to those of “upward (downward) peaks of isotherms” observed by Ozawa and Kawamoto [16] and the temperature “annular effects” observed by Zhao and Cheng [17]. The results shown in Figs. 6 and 7 also suggest that the steeper the temperature gradient, the stronger the temperature overshoot/undershoot effects become. Furthermore, if there is no temperature gradient, temperature undershoot/overshoot effects will not occur. This is similar to findings of Zhao and Cheng [17], namely that there is not temperature “annular effect” in the middle of their heated pipe when no temperature gradient exists.

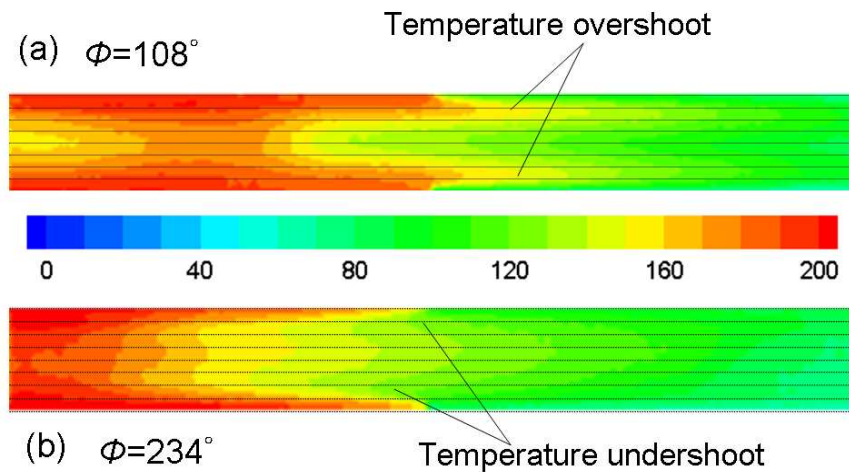


Figure 12 Temperature fields for (a) $\phi = 108^\circ$, and (b) $\phi = 234^\circ$; the distance between two neighbouring grid lines is 0.75 mm. (temperature scale in degrees Celsius)

3.5.2 Considerations of the effect of "flow history" on the oscillatory flow behaviour

An interesting observation that can be made in Fig. 4 is that, although the gas nearly reaches the equilibrium position in both phases $\phi = 90^\circ$ and $\phi = 270^\circ$, the temperature fields at these two phases are clearly different. One can also compare phases $\phi = 54^\circ$ and $\phi = 306^\circ$ in which the gas parcel is nearly in the same position. However, there is a clear temperature overshoot effect at phase $\phi =$

54° but not at phase $\phi = 306^\circ$. Other pairs of such images can also be compared. This illustrates simply the fact that the flow history (i.e. temperature distribution within the fluid in all preceding phases) determines the pattern of temperature distribution at the phase of interest.

However, despite the unique and complicated characteristics of oscillatory flows, the engineering design of the heat exchangers for oscillatory situations uses results and data from research in steady flows, because there are few relevant experimental and numerical studies made in oscillatory flows, and those available are not being widely used due to their fragmentary character.

One of the typical approaches is to use the steady flow correlations available to determine the heat transfer coefficient in order to estimate the time averaged temperature difference between the oscillating gas and solid surface, using RMS value of Reynolds number as an input for the calculations [29]. Such treatment is based on the so-called Iguchi hypothesis, i.e. that each instant of the time-dependent flow depends only on that instant's velocity, not on the flow history. However, the experimental results such as these presented here show that the Iguchi hypothesis is invalid for heat transfer process in the oscillatory flow and therefore the current design procedures and calculations are strictly not suitable.

3.5.3 Effects of temperature overshoot/undershoot on the heat transfer

According to Fig. 6, the difference between the temperature peak and the temperature of gas in the channel centre or at the wall is in the order of tens of degrees Celsius. These temperature differentials clearly exist within the transverse distances in the order of $\delta_{v,a}$. Therefore, the transverse temperature gradients caused by these temperature differences are in the order of 10,000 °C/m, which is very high. They lead to the transverse heat exchange processes between gas layers and this is the mechanism behind enhancing the transverse heat transfer between the plate surface and the gas. Furthermore, the inhomogeneous temperature profiles also enhance the axial heat transfer along the channel. This type of heat transfer enhancement is beneficial for heat exchangers subjected to oscillatory flow.

In thermal buffer tubes of thermoacoustic engines, and pulse tubes of pulse tube coolers, a large temperature difference is produced by ways such as mechanical power input and is required to be maintained by virtue of stratified flow and ideally linear temperature distribution [29]. Such inhomogeneous temperature profiles and temperature undershoots and overshoots are likely to

increase the heat transfer along the temperature gradient and will inevitably lead to heat (or cooling) losses.

On the other hand, the results obtained in this work show on the microscopic level of individual flow channels that the gas outside $y > 2.5\delta_\kappa$ is practically not affected by the thermal diffusion from the channel wall. The heat exchangers to be used in oscillatory flow often require a greater heat transfer area for a given overall size. Hence, advised by this analysis, the distance between the solid heat transfer surfaces, such as fins, could be around 4–5 times δ_κ to keep the heat transfer surfaces closely packed, while not at a cost of much greater pressure drop due to the viscous losses.

4. Numerical simulation and results

The oscillatory flow produced in the current experimental apparatus is limited to a single frequency and one oscillation amplitude. To overcome this shortcoming, the computational tool was introduced to extend the examination discussed above to a range of frequencies and oscillation amplitudes. The details of the numerical scheme are available in [33]. The complete set of continuity, momentum and energy equations is solved over a computational domain that covers the pair of heat exchangers and a length of 270 mm either way from the joint of hot and cold plates. The same geometrical configuration as that used in the experiments is adopted. The boundary conditions for the inlet and outlet of the domain are pre-defined [31], with the resonator wall set as adiabatic. The temperature distribution on the surface of the heat exchanger plates is introduced into the computational model. The modelled operating conditions are listed in Table 1, all at atmospheric pressure. The simulation was validated by comparing the flow fields against the experimental results and a good agreement was reached (omitted here for brevity). According to the investigation in [31], laminar model is recommended when the displacement amplitude is small, such as 17 mm, and the two-equation SST $k-\omega$ turbulence model should be used when the displacement amplitude is higher.

Table 1 Operating conditions used in the numerical simulation

Cases	Frequency (Hz)	Displacement amplitude (mm)	Womersley number, α	Kinematic Reynolds number, Re_ω
1	13.1	17	9.2 - 13.4	85 - 180
2	13.1	35	9.2 - 13.4	85 - 180
3	13.1	50	9.2 - 13.4	85 - 180
4	25	8.9	12.7- 18.6	162 - 345
5	50	4.5	18.0-26.3	325 - 690

The temperature profiles at $x = 5.0$ mm for ten selected phases are given in Fig. 13, when the displacement amplitude is 17 mm, 35 mm and 50 mm respectively. The temperature profiles for $\xi_a = 17$ mm is in general in agreement with the experimental results. The “temperature overshoot” is clearly visible, in particular for $\phi = 54$ – 126° . The effect of heat diffusion reaches beyond $3\delta_{v,a}$, which is quite different from the experimental observation. The actual reason remains unclear. The gas temperature at the centre of the channel is higher in the numerical results, compared with the measurements, especially at $\phi = 342^\circ$ and 18° . This could be caused by the settings of the thermal boundary conditions in the simulation, where the excessive heat can only leave the computational domain through the inlet and outlet.

While the gas is subject to different excitation levels, the oscillatory flow shares the same Womersley number due to the same frequency. Hence the Stokes’ boundary layer thickness is also the same. However, it can be seen in Fig. 13 that the temperature peaks appear close to the cold plate, when the displacement amplitude, thus the velocity amplitude, is bigger. Nevertheless, the temperature overshoot effect is still clearly visible. The temperature peak moving closer to the solid wall is understood to be caused by the change of the viscous boundary layer. Similar observation is made in the hot channel.

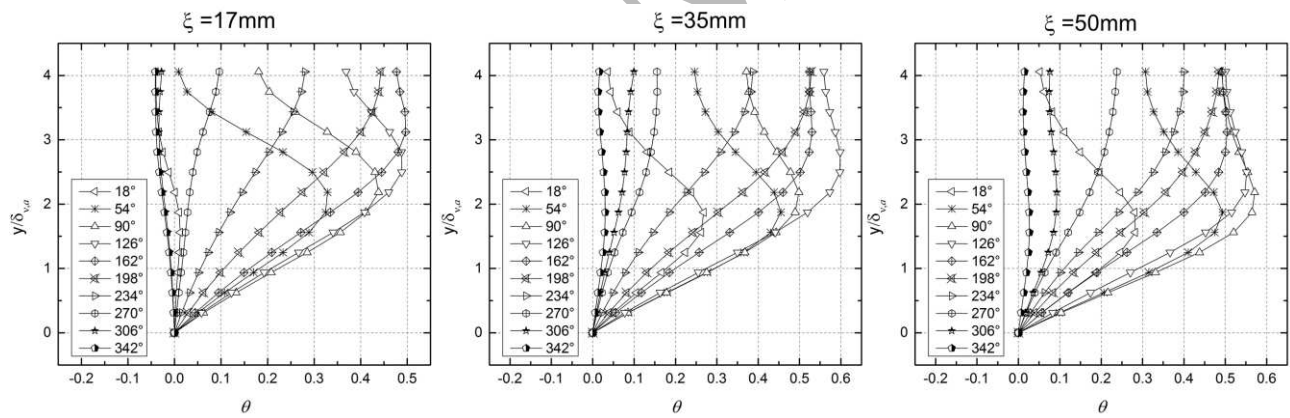


Figure 13 Cross-sectional temperature profiles for ten selected phases ($x=5.0$ mm) at different oscillation amplitudes ($f = 13.1\text{Hz}$)

Under the investigated frequencies (13.1–50 Hz), the velocity amplitude in the flow channel is kept constant. Hence, the displacement amplitude decreases when the operating frequency increases. The Womersley number of the oscillatory flow covers a range of 9.2–26.3. The temperature profiles at $x = 5.0$ mm for ten selected phases are given in Fig. 14, when the operating frequency changes to 25 Hz and 50 Hz. The temperature overshoot effect is still clearly present. The temperature peaks are located around $2\delta_{v,a}$ from the solid wall and the magnitude of the temperature overshoot reduces with the increase of frequency. So is the change of the gas temperature at the centre of the channel.

These are considered to be controlled by the displacement that the gas can travel within a cycle. For a smaller displacement, the temperature change that gas can experience will be smaller, even if the temperature gradient is maintained the same.

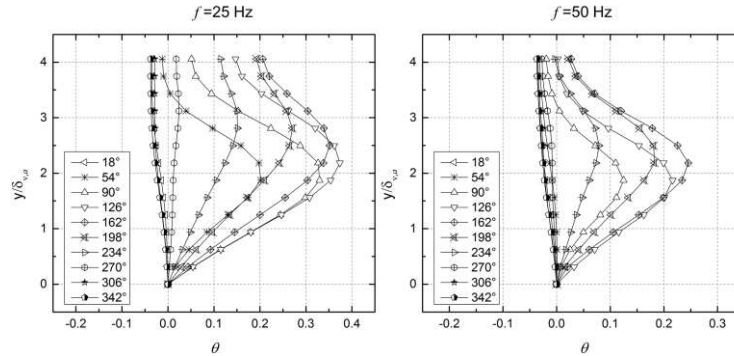


Figure 14 Cross-sectional temperature profiles for ten selected phases ($x=5.0$ mm) at different operating frequencies

5. Conclusion

This paper investigates the interaction between thermal and viscous boundary layers in a channel with a nonlinear temperature gradient. The mechanism of the heat transfer associated with the oscillatory flow has been analysed in detail. The phase lag between different layers of gas adjacent to the wall leads to large transverse temperature gradient normal to the plate surface, which gives rise to the temperature undershoot and overshoot phenomena in this research. These time dependent transverse temperature gradients enhance the heat transfer between the gas and plates, as well as the heat transfer along the channel. Furthermore, the experimental results indicate that the flow history at the preceding phases would significantly affect the temperature distribution at subsequent phases. This indicates the Iguchi hypothesis, which enables the application of the heat transfer data for steady flows to the oscillatory flow conditions, may not always be reliable, at least at the conditions studied in this work.

Acknowledgments

Artur J. Jaworski would like to acknowledge the support for his research programme in fundamentals of thermoacoustics received from EPSRC under grants GR/S26842/01GR/T04502/01, GR/T04519/01, EP/E044379/1 and EP/E044379/2 and thus for creating research training opportunities for Drs Mao and Yu. Dr Lei Shi is acknowledged for his expert PIV and PLIF measurements under the supervision of Dr Mao and data processing required to produce illustrative material. Dr. Fatimah A.Z. Mohd Saat provided support on the numerical simulation.

References

1. Kaviany M and Reckker M, Performance of a heat exchanger based on enhanced heat diffusion in fluids by oscillation: experiment, *Journal of Heat Transfer*, 112 (1) (1990) 56-63.
2. Liao QD, Yang KT and Nee VW, Enhanced microprocessor chip cooling by channelled zero-mean oscillatory air flow, in: Hsu TR et al (Ed.), *Proceedings of the International Intersociety Electronic Packaging Conference, Advances in Electronic Packaging, EEP-Vol.10-2*, ASME, NY, 1995, pp. 789–794.
3. Beskok A and Warburton TC, Arbitrary Lagrangian Eulerian analysis of a bidirectional micro-pump using spectral elements, *International Journal Computational Engineering Science*, 2(1) (2001) 43–57.
4. Oddy MH, Santiago JG and Mikkelsen JC, Electrokinetic instability micromixing, *Analytical Chemistry*, 73(24) (2001) 5822–5832.
5. Sert C and Beskok A, Oscillatory flow forced convection in micro heat spreaders, *Numerical Heat Transfer, Part A*. 42(7) (2002) 685–705.
6. Paek I, Braun JE and Mongeau L, Characterizing heat transfer coefficients for heat exchangers in standing wave thermoacoustic coolers, *Journal of the Acoustical Society of America*, 118 (4) (2005) 2271-2280.
7. Nsofor EC, Celik S and Wang X, Experimental study on the heat transfer at the heat exchanger of the thermoacoustic refrigerating system, *Applied Thermal Engineering*, 27 (14-15) (2007) 2435-2442.
8. Wakeland RS and Keolian RM, Calculated effects of pressure-driven temperature oscillations on heat exchangers in thermoacoustic devices with and without a stack, *Journal of the Acoustical Society of America*, 116 (1)(2004) 294-302.
9. Cooper WL, Nee VW and Yang KT, Fluid mechanics of oscillatory and modulated flows and associated applications in heat and mass transfer – a review, *Journal of Energy, Heat and Mass Transfer*, 15 (1993) 1-19
10. Zhao TS and Cheng P, Heat transfer in oscillatory flows, *Annual Review of Heat Transfer*, Tien C-L (Ed.), IX (Chapter 7) (1998)
11. Sert C and Beskok A, Numerical simulation of reciprocating flow forced convection in two-dimensional channels, *Journal of Heat Transfer*, 125 (2003) 403-412.
12. Kurzweg UH and Zhao LD, Heat transfer by high-frequency oscillations: a new hydrodynamic technique for achieving large effective thermal conductivities, *Physics of Fluids*, 27 (11) (1984) 2624-2627.

13. Kurzweg UH, Temporal and spatial distribution of heat flux in oscillating flow subjected to an axial temperature gradient, *International Journal of Heat and Mass Transfer*, 29 (12) (1986) 1969-1977.
14. Kurzweg UH, Enhanced heat conduction in fluids subjected to sinusoidal oscillations, *Journal of Heat Transfer*, 107 (2) (1985) 459-462.
15. Zhao AX and Kurzweg UH, Extension of the SIMPLE algorithm to heat transfer in time-periodic flows with moving boundaries, *Numerical Heat Transfer, Part B*, 18 (1990) 189-203.
16. Ozawa M and Kawamoto A, Lumped-parameter modelling of heat transfer enhanced by sinusoidal motion of fluid, *International Journal of Heat and Mass Transfer*, 34 (12) (1991) 3083-3095.
17. Zhao TS and Cheng P, A numerical solution to laminar forced convection in a heated pipe subjected to a reciprocating flow, *International Journal of Heat and Mass Transfer*, 38 (16) (1995) 3011-3022.
18. Li P and Yang KT, Mechanisms for the heat transfer enhancement in zero-mean oscillatory flows in short channels, *International Journal of Heat and Mass Transfer*, 43 (2000) 3551-3566.
19. Mozurkewich G, Heat transfer from a cylinder in an acoustic standing wave, *Journal of the Acoustical Society of America*, 98(4) (1995) 2209-2216.
20. Leong KC and Jin LW, An experimental study of heat transfer in oscillating flow through a channel filled with an aluminium foam, *International Journal of Heat and Mass Transfer*, 48 (2005) 243-253.
21. Leong KC and Jin LW, Heat transfer of oscillating flow and steady flows in a channel filled with porous media, *International Communication of Heat and Mass Transfer*, 31 (2004) 63-72.
22. Ozawa M, Shinoki M, Nagoshi K and Serizawa E, Scaling of heat transfer characteristics in an oscillating flow, *Journal of Enhanced Heat Transfer*, 10(3) (2003) 275-285.
23. Wetzel M and Herman C, Experimental study of thermoacoustic effects on a single plate part II: heat transfer, *Heat and Mass Transfer*, 35 (6) (1999) 433-441.
24. Wetzel M and Herman C, Experimental study of thermoacoustic effects on a single plate part I: temperature fields, *Heat and Mass Transfer*, 36 (1) (2000) 7-20.
25. Peattie RA and Budwig R, Heat transfer in laminar, oscillatory flow in cylindrical and conical tubes, *International Journal of Heat and Mass Transfer*, 32 (5) (1989) 923-934.
26. Shi L, Mao X and Jaworski AJ, Application of planar laser induced fluorescence measurement techniques to study heat transfer characteristics of parallel-plate heat exchangers in thermoacoustic devices, *Measurement Science and Technology*, 21(11) (2010) 115405 (16pp).

27. Mao X and Jaworski AJ, Application of particle image velocimetry measurement techniques to study turbulence characteristics of oscillatory flows around parallel-plate structures in thermoacoustic devices, *Measurement Science and Technology*, 21(3) (2010) 035403 (16pp).
28. Swift GW, Thermoacoustic engines, *Journal of the Acoustical Society of America*, 84 (1988) 1145-1180.
29. Swift GW, *Thermoacoustics: A unifying perspective for some engines and refrigerators*, Acoustical Society of America, New York (2002).
30. Iguchi M, Ohmi M and Maegawa K, Analysis of free oscillating flow in a U-shaped tube, *Bulletin of the JSME*, 25(207) (1982), 1398-1405.
31. Petculescu A and Wilen LA, Oscillatory flow in jet pumps: Nonlinear effects and minor losses, *Journal of the Acoustical Society of America*, 113(3) (2003), 1282-1292.
32. Rott N, Damped and thermally driven acoustic oscillations in wide and narrow tubes, *Zeitschrift für Angewandte Mathematik und Physik*, 29 (1969) 230–243.
33. MohdSaad FAZ and Jaworski AJ, Oscillatory flow and heat transfer within parallel-plate heat exchangers of thermoacoustic systems, *Proceedings of the World Congress on Engineering (WCE)*, Vol. III, July 3-5, 2013, London, UK.